ORIGINAL ARTICLE

Gait speed and spasticity are independently associated with estimated failure load in the distal tibia after stroke: an HR-pQCT study

Tiev Miller[1] · Ling Qin[2] · Vivian W. Y. Hung[2] · Michael T. C. Ying[3] · Charlotte S. L. Tsang[1] · Huixi Ouyang[1] · Raymond C. K. Chung[1] · Marco Y. C. Pang[1]

Abstract

Summary This HR-pQCT study was conducted to examine bone properties of the distal tibia post-stroke and to identify clinical outcomes that were associated with these properties at this site. It was found that spasticity and gait speed were independently associated with estimated failure load in individuals with chronic stroke.

Purpose (1) To examine the influence of stroke on distal tibia bone properties and (2) the association between these properties and clinical outcomes in people with chronic stroke.

Methods Sixty-four people with stroke (age, 60.8 ± 7.7 years; time since stroke, 5.7 ± 3.9 years) and 64 controls (age: 59.4 ± 7.8 years) participated in this study. High-resolution peripheral quantitative computed tomography (HR-pQCT) was used to scan the bilateral distal tibia, and estimated failure load was calculated by automated finite element analysis. Echo intensity of the medial gastrocnemius muscle and blood flow of the popliteal artery were assessed with ultrasound. The 10-m walk test (10MWT), Fugl-Meyer Motor Assessment (FMA), and Composite Spasticity Scale (CSS) were also administered.

Results The percent side-to-side difference (%SSD) in estimated failure load, cortical area, thickness, and volumetric bone mineral density (vBMD), and trabecular and total vBMD were significantly greater in the stroke group than their control counterparts (Cohen's $d = 0.48$–1.51). Isometric peak torque and echo intensity also showed significant within- and between-groups differences ($p \leq 0.01$). Among HR-pQCT variables, the %SSD in estimated failure load was empirically chosen as one example of the strong discriminators between the stroke group and control group, after accounting for other relevant factors. The 10MWT and CSS subscale for ankle clonus remained significantly associated with the %SSD in estimated failure load after adjusting for other relevant factors ($p \leq 0.05$).

Conclusion The paretic distal tibia showed more compromised vBMD, cortical area, cortical thickness, and estimated failure load than the non-paretic tibia. Gait speed and spasticity were independently associated with estimated failure load. As treatment programs focusing on these potentially modifiable stroke-related impairments are feasible to administer, future studies are needed to determine the efficacy of such intervention strategies for improving bone strength in individuals with chronic stroke.

Keywords Failure load · HR-pQCT · Stroke · Tibia

✉ Marco Y. C. Pang
marco.pang@polyu.edu.hk

Tiev Miller
tiev.b.miller@connect.polyu.hk

Ling Qin
lingqin@cuhk.edu.hk

Vivian W. Y. Hung
vivi@cuhk.edu.hk

Michael T. C. Ying
michael.ying@polyu.edu.hk

Charlotte S. L. Tsang
charlotte.tsang@connect.polyu.hk

Huixi Ouyang
huixi.ouyang@connect.polyu.hk

Raymond C. K. Chung
raymond.ck.chung@polyu.edu.hk

[1] Department of Rehabilitation Sciences, The Hong Kong Polytechnic University, Hung Hom, Hong Kong

[2] Bone Quality and Health Centre, Department of Orthopaedics and Traumatology, The Chinese University of Hong Kong, Sha Tin, Hong Kong

[3] Department of Health Technology and Informatics, The Hong Kong Polytechnic University, Hung Hom, Hong Kong

Introduction

The skeletal system endures considerable change after stroke [1], with declines in bone strength identified as a major risk factor for fracture [2]. Although fracture risk has been shown to increase after stroke [3, 4], preventative measures for reducing bone loss in the chronic stages of stroke are often underemphasized during recovery [2]. Thus, factors influencing bone loss, and consequently bone strength, are of particular relevance for individuals with chronic stroke [1].

Previous studies have examined paretic lower limb bone status using either peripheral quantitative computed tomography (pQCT) or dual-energy X-ray absorptiometry (DXA) [5–12]. A consistent finding is lower cortical bone mineral density (BMD) and compromised bone geometry of the paretic tibia. DXA provides clinically relevant assessment of areal BMD post-stroke [12, 13] but lacks the sensitivity to evaluate compartmental bone segments independently [14]. Although more often used for research purposes, pQCT scans not only provide an assessment of bone density and but also geometry [5, 7], an important determinant of bone strength [14]. A limitation of the earlier pQCT studies was the inability to examine bone microstructure, which is relevant to the investigation of bone fragility [15]. Microstructure [16–19] and estimated bone strength [17, 19, 20] of the tibia, which can be assessed using high-resolution peripheral quantitative computed tomography (HR-pQCT) and micro-finite element (µFE) analysis, have been shown to be important determinants of incident fracture [21].

A recent study using HR-pQCT to examine the impact of stroke on volumetric bone mineral density (vBMD), area, and microstructure of the distal tibia found a significant reduction in these outcomes for the paretic side relative to the non-paretic side within the first 6 months following stroke onset (i.e., acute and subacute stages of stroke recovery) [22]. The degree of functional motor recovery determined with the Chedoke-McMaster Stroke Assessment was also correlated with the percent change in total vBMD for the paretic distal tibia at 6 months post-stroke. However, the sample size was small (i.e., 22 participants with stroke). The association between modeled estimates of mechanical bone strength (i.e., µFE derived data) and clinically relevant measures of dysfunction and impairment after stroke was not assessed. Moreover, bilateral limb differences in HR-pQCT bone outcomes for people with stroke relative to matched groups without prior stroke history were not compared.

The first objective of this HR-pQCT study was to examine the impact of stroke on the bone properties of the distal tibia. Our second objective was to then determine the association between these properties and clinically relevant measures of functional impairment in people with chronic stroke (> 6 months post onset). Given there are numerous cofactors influencing bone metabolism (i.e., genetic, age, sex, nutrition), it is important to identify the stroke-specific factors associated with bone status, as these may serve as potential intervention targets. A similar approach has been used in a previous HR-pQCT study involving the distal radius in people with chronic stroke [23]. It was hypothesized that compromised bone status would be more evident on the paretic side in comparison to the non-paretic side and control participants. It was also hypothesized that the side-to-side difference in bone parameters would be significantly correlated with stroke-related lower limb motor impairment.

Methods

Participants

Individuals with chronic stroke and age- and sex-matched controls without prior stroke history were recruited through convenience sampling. Recruitment occurred between April 11, 2018, and February 28, 2019. The study was approved by the Human Subjects Ethics Sub-committee of the University (reference number HSEARS20171212003 on January 2, 2018) and the Clinical Research Ethics Committee of the hospital on April 10, 2018 (reference number 2017–711). Prior to data collection, informed consent was obtained for all participants. Assessment procedures were conducted according to the Helsinki Declaration for human experiments.

Inclusion and exclusion criteria

The inclusion criteria for the stroke group were (1) history of chronic stroke (onset > 6 months), (2) > 18 years of age, (3) residing within the local community, and (4) ability to achieve 0° of passive ankle plantar-dorsiflexion required for conducting ultrasound and isometric strength assessments. Stroke group exclusion criteria were (1) diagnoses of other neurological conditions; (2) musculoskeletal conditions, disorders, or dysfunctions (e.g., limb amputation); (3) metal implants at the distal tibia; (4) lower extremity fracture within the previous 12 months; (5) prior diagnosis of osteoporosis; and (6) other serious illnesses that precluded study participation. The control group eligibility criteria were the same with the exception of previous stroke history.

Procedures

Bone imaging was conducted at a bone imaging center in a local hospital. HR-pQCT (XtremeCT II, Scanco Medical AG, Brüttisellen, Switzerland) was used to measure bone properties of the bilateral distal tibia. All variables collected are described in Supplemental Table 1 and are categorized in accordance with recent guidelines [24]. A description of the scanning procedures as well as the standard 3D and µFE analyses performed are provided in Supplemental Appendix 1. Ultrasound measurement procedures involving the use of B-mode (i.e., echo intensity) and pulse wave Doppler (i.e., peak systolic velocity) are described in Supplemental Appendix 2. A description of stroke-specific assessments (i.e., stroke characteristics, motor function using the Fugl-Meyer Assessment (FMA), and scores of spasticity using the Composite Spasticity Scale (CSS)) is provided in Supplemental Appendix 3. All other functional assessments (i.e., Physical Activity Scale for the Elderly (PASE), 10-m walk test (10MWT), plantar flexor isometric peak torque, touch pressure threshold) are described in Supplemental Appendix 4.

Statistical analysis

A priori power analyses conducted were based on findings from the previous pQCT studies of the distal tibia in people with stroke [7, 10] and are described in Supplemental Appendix 5. SPSS (version 26, IBM Corp., Armonk, New York, USA) was used for the following analyses (two-tailed). Normality was determined using the Kolmogorov–Smirnov test, and homogeneity was examined using the Levene's test. Independent t, Mann–Whitney U, and χ^2 tests were used in comparing baseline between-group differences for participant characteristics according to continuous, ordinal, and nominal levels of data, respectively. Paired t-tests were used to compare differences between sides (paretic vs non-paretic (stroke group), non-dominant vs dominant (control group)), and independent t-tests were used to compare the percent side-to-side difference (%SSD) between groups (stroke vs control) for all HR-pQCT, ultrasound, and functional impairment outcomes measured bilaterally. The alpha level was adjusted according to the number of comparisons made (i.e., Bonferroni correction; 3 comparisons, adjusted alpha = 0.017). Standardized effect sizes for within- and between-group differences were reported as Cohen's d. Values ranging from 0.00 to 0.20, 0.20–0.50, 0.50–0.80, and > 0.80 represent very small, small, medium, and large effect sizes, respectively [25]. To calculate %SSD for each variable measured bilaterally, the following formula was used:

$$\frac{\text{Non-paretic or Dominant side} - \text{Paretic or Non-dominant side}}{\text{Non-paretic or Dominant side}} \times 100$$

In order to establish which bone parameters most accurately determined participant classification to either the stroke or control group, discriminant analyses were first conducted for each HR-pQCT variable. Group classification was used as the categorical dependent variable (0 = control, 1 = stroke), and bone variables (%SSD) were then entered separately as independent factors. Next, other factors of physiological relevance (i.e., sex, age, BMI, PASE, calcium supplementation, tobacco use, alcohol consumption, total number of comorbidities, and medications) were also entered into the model.

For the stroke group, bivariate correlation analyses (Pearson's r) were used to determine the association between the dependent variable and %SSD or raw values of all other continuous variables. Relationships between variables were defined as having minimal or no correlation ($r = 0.00$–0.25), fair ($r = 0.25$–0.50), moderate to strong ($r = 0.50$–0.75), or very strong correlation ($r > 0.75$) [25]. For categorical variables, Mann–Whitney U tests were used to compare differences in the dependent variable for subgroups categorized according to alcohol, tobacco, and supplement usage. To determine the time-dependent effect of stroke on HR-pQCT variables, ultrasound, and functional variables assessed bilaterally, a set of subgroup analyses were performed for dichotomous groups of above or below average time since stroke (i.e., 5.8 ± 4.0 years) and for tertile groups of comparable numbers (group 1 ≤ 3 years, group 2 = 4–5 years, and group 3 ≥ 6 years since stroke). Associations between time since stroke and other variables were assessed using Pearson's r correlations. Differences between groups were determined using independent t-tests for dichotomous groups and one-way ANOVA for tertile groups. A similar analysis approach has been used previously [23].

Based on the results generated from the above analyses, %SSD in estimated failure load was empirically selected as one example of the strong discriminators between the stroke group and control group, and then used as the dependent variable in the subsequent hierarchical multiple regression analysis. The regression analysis was used to determine which stroke-related impairments showed the strongest associations with %SSD in estimated failure load among individuals with stroke. Factors of physiological relevance (e.g., age, sex, BMI, PASE, etc.) were first entered into the model in one block (i.e., base model). Next, those stroke impairment variables demonstrating significant results in the bivariate correlation analysis were then entered into the model using the stepwise method. A separate set of correlations were performed prior to the regression analysis to test the association among predictors (independent variables). To avoid multicollinearity, highly correlated predictors (i.e., $r \geq 0.6$) would be placed in separate models [26]. The level of significance was set at 0.05 for correlation and regression analyses.

Results

Participant characteristics

Prior to data collection, 67 individuals with stroke and 66 healthy controls were screened by phone between June 1, 2018, and March 30, 2019. Among the participants with stroke, an individual was excluded due to a congenital bone deformation of the tibia, and two others withdrew of their own volition prior to completing all assessments. Among the controls, an individual was excluded for an Achilles tendon repair and another for an essential tremor. A total of 128 participants (64 strokes, 64 controls) were assessed. Motion grade scores for all participant bone scans were of adequate quality (≤ 3) with no significant differences between limbs or groups (Supplemental Table 2). Participant characteristics are summarized in Table 1. Significant between-group differences were observed for gait velocity (10MWT), total number of comorbidities, and medications ($p \leq 0.01$). The mean scores for FMA (26.7 ± 4.4) and CSS (7.1 ± 2.6) indicated that participants with stroke had moderate motor impairment and mild spasticity, respectively.

HR-pQCT

Not all variables met the criteria for normality. As the sample size was decent and equal between groups, the analysis chosen was considered robust [27]. A summary of the analysis results for HR-pQCT variables is provided in Table 2. Bilateral comparisons between HR-pQCT images of the distal tibia taken from representative participants in the stroke and control groups are provided in Fig. 1.

Significant paired *t*-tests indicate that the paretic limbs had lower estimated failure load, cortical area, cortical thickness, total vBMD, cortical vBMD, and trabecular vBMD compared to non-paretic limbs (Cohen's $d = 0.16$–0.45). No significant between-sides differences were observed for controls.

Independent *t*-tests also showed larger %SSD in the aforementioned variables for the stroke group compared to controls. Effect estimates for between-group differences were large (Cohen's $d = 1.25$–1.51), with the exception of %SSD in trabecular vBMD (Cohen's $d = 0.48$).

Ultrasound and functional measures

Paretic limbs had significantly higher echo intensity, lower isometric peak torque, and higher touch pressure threshold in comparison to non-paretic limbs. No significant

between-sides differences were observed for controls. The stroke group also showed significantly greater %SSD in echo intensity and isometric peak torque than controls (Supplemental Table 3).

Discriminant analyses

The results indicated greater classification accuracy for cortical vBMD, cortical area, cortical thickness, and estimated failure load in differentiating between stroke and control groups relative to other HR-pQCT variables (75%) (Supplemental Table 4, Summary 1). Estimated failure load in combination with other physiologically relevant factors yielded a classification accuracy of 84.4% (Table 3, Model 2).

Correlations and subgroup analyses

Among the functional impairment variables, CSS-ankle clonus ($r = 0.289$, $p = 0.020$), FMA ($r = -0.252$, $p = 0.045$), and 10MWT ($r = -0.319$, $p = 0.010$) showed fair associations with %SSD in estimated failure load. In contrast, no significant correlations were found between %SSD in cortical vBMD and functional impairment variables (Supplemental Table 5).

Mann–Whitney *U* test results showed no significant differences for %SSD in estimated failure load for subgroups according to alcohol, tobacco, calcium, and vitamin D supplement usage ($p \leq 0.811$).

Correlations between time since stroke and HR-pQCT, ultrasound, and functional impairment variables are provided in Supplemental Table 6. Only the %SSD in trabecular number showed a fair association with time since stroke ($r = -0.262$, $p = 0.036$). No significant between-group differences were found for HR-pQCT, ultrasound, or functional variables based on below (≤ 5 years) or above average time since stroke (> 5 years) ($p \leq 0.895$). For tertile subgroups of comparable numbers, only %SSD in cortical perimeter showed a significant between-groups difference ($F = 3.872$, $p = 0.026$), with larger %SSD for group 1 (≤ 3 years since stroke, $n = 19$, 0.74 ± 1.32) and group 3 (≥ 6 years since stroke, $n = 24$, 0.67 ± 2.09) compared to group 2 (4–5 years since stroke, $n = 21$, 0.52 ± 1.28).

Regression

Based on HR-pQCT variable comparisons (Table 2), group classification accuracy (Supplemental Table 4), and correlation results (Supplemental Table 5), estimated failure load was empirically selected as one example among the strong discriminators between the stroke group and control group, and was therefore used as the dependent variable in the regression analysis. A high degree of

Table 1 Participant characteristics

	Stroke ($N=64$)	Control ($N=64$)	p
Demographics			
Sex (men/women), n	38/26	39/25	0.858
Age (years)	60.8 ± 7.7	59.4 ± 7.8	0.306
Menopause (women), years	12.4 ± 13.1	11.5 ± 9.9	0.787
BMI (kg/m^2)	24.3 ± 3.1	23.4 ± 2.8	0.081
Leg dominance (left/right/equivalent), n	5/56/3	2/62/0	0.101
Alcohol consumption (drinks/day)	0.2 ± 0.3	0.1 ± 0.3	0.276
Tobacco use (packs/day)	0.7 ± 0.4	0.6 ± 0.3	0.428
Daily vitamin D supplementation (yes/no), n	4/60	4/60	1.000
Daily calcium supplementation (yes/no), n	3/61	7/57	0.188
PASE	114.7 ± 87.4	142.2 ± 79.4	0.065
10MWT velocity (m/s)	0.81 ± 0.39	1.87 ± 0.31	<0.001[*]
Stroke characteristics			
Paretic side (left/right), n	36/28	-	-
Total number of strokes (1/2), n	63/1	-	-
Type of stroke (ischemic/hemorrhagic), n	41/23	-	-
Time since stroke, years	5.8 ± 4.0	-	-
Stroke location (ACS/ PACS/ LS/ PCS/ hemorrhagic)	8/22/10/1/23	-	-
CSS-Achilles tendon jerk (0–4)	1.7 ± 0.8	-	-
CSS-resistance to displacement (0–8)	4.1 ± 2.0	-	-
CSS-ankle clonus (1–4)	1.3 ± 0.6	-	-
CSS-lower limb total (1–16)	7.1 ± 2.6	-	-
FMA-lower extremity (0–34)	26.7 ± 4.4	-	-
Comorbidity			
Total number of comorbidities, n	1.3 ± 1.3	0.6 ± 0.9	<0.001[*]
Hypertension, n	37	22	0.006[*]
Hyperlipidemia, n	21	4	<0.001[*]
Cardiac arrhythmia, n	1	0	0.315
Diabetes mellitus, n	14	8	0.150
Ischemic heart disease, n	1	0	0.315
Medication			
Total number of medications, n	4.0 ± 2.7	0.8 ± 1.2	<0.001[*]
Antihypertensive agents, n	42	16	<0.001[*]
Hypolipidemic agents, n	41	10	<0.001[*]
Hypoglycemic agents, n	10	6	0.259
Anticoagulants, n	23	3	<0.001[*]
Antispasmodic agents, n	6	0	0.011[*]
Cardiac medication/ agent, n	4	0	0.039[*]

[*]$p \leq 0.05$ statistically significant difference between groups

Abbreviations: *BMI* body mass index, *PASE* Physical Activity Scale for the Elderly, *10MWT* 10-m walk test, *ACS* anterior circulation syndrome, *PACS* partial anterior circulation syndrome, *LS* lacunar syndrome, *PCS* posterior circulation syndrome, *CSS* Composite Spasticity Scale, *FMA* Fugl-Meyer Assessment

multicollinearity was not evident among independent predictor variables selected for inclusion in the regression analysis ($r = -0.007$ to -0.478) (Supplemental Table 7). After accounting for other relevant factors, the 10MWT (model 3: $\beta = -0.331$, $p = 0.009$) and CSS-ankle clonus (model 3: $\beta = 0.239$, $p = 0.032$) were independently associated with the %SSD in estimated failure load (model 3: $F = 3.510$, $p = 0.001$), accounting for 9.4% and 5.0% of the variance, respectively. The FMA-LE was eliminated as a predictive factor in the stepwise model. Overall, the final model (model 3) explained approximately 50.1% of the variance in %SSD of estimated failure load (Table 4).

Table 2 Comparison of HR-pQCT variables between stroke and control groups

	Stroke (N=64)			Control (N=64)			Side effect (Within—stroke)			Side effect (Within—control)			%SSD effect (Between groups)		
	Paretic	Non-paretic	SSD (%)	Non-dominant	Dominant	SSD (%)	t	p	d	t	p	d	t	p	d
Volumetric density and area															
Total vBMD (mg HA/cm³)	255.42±64.63	277.45±55.77[a]	8.7±8.2[b]	285.12±51.99	286.29±53.32	0.2±5.0	−9.0	<0.001	0.36	−0.6	0.508	0.02	−7.0	<0.001	1.25
Cortical vBMD (mg HA/cm³)	809.46±82.17	843.20±66.12[a]	4.1±3.8[b]	872.10±57.32	871.76±56.25	−0.1±1.9	−9.0	<0.001	0.45	0.1	0.868	0.00	−7.8	<0.001	1.39
Trabecular vBMD (mg HA/cm³)	145.40±39.81	151.50±35.10[a]	4.7±11.0[b]	147.30±35.32	147.61±33.60	0.3±6.3	−3.3	0.002	0.16	−0.2	0.791	0.00	−2.7	0.007	0.48
Cortical area (mm²)	109.53±32.08	122.56±29.19[a]	11.6±9.2[b]	131.94±24.64	132.42±25.59	−0.01±5.7	−10.2	<0.001	0.42	−0.5	0.597	0.01	−8.5	<0.001	1.51
Trabecular Area (mm²)	578.64±138.73	571.38±137.71	−1.4±4.9	576.51±133.86	577.68±135.11	−0.03±4.6	2.1	0.033	0.05	−0.3	0.714	0.00	1.6	0.107	0.28
Cortical microstructure															
Cortical thickness (mm)	1.28±0.37	1.43±0.33[a]	10.9±10.4[b]	1.50±0.27	1.51±0.30	−0.3±6.5	−9.1	<0.001	0.42	−0.3	0.718	0.03	−7.3	<0.001	1.29
Cortical perimeter (mm)	102.23±10.60	102.51±10.55	0.3±1.7	103.33±10.40	103.45±10.42	0.1±1.8	−1.2	0.211	0.02	−0.5	0.617	0.01	−0.5	0.564	0.10
Intracortical porosity (%)	0.039±0.017	0.036±0.014	−11.9±36.1	0.033±0.015	0.032±0.015	−7.8±39.4	1.7	0.078	0.19	0.9	0.322	0.06	0.6	0.532	0.11
Trabecular microstructure															
Trabecular number (1/mm)	1.12±0.17	1.13±0.15	0.9±6.6	1.10±0.17	1.11±0.16	1.0±4.8	−0.9	0.324	0.06	−1.7	0.081	0.06	0.0	0.961	0.01
Trabecular thickness (mm)	0.25±0.02	0.26±0.02	0.6±4.4	0.26±0.02	0.25±0.02	−0.3±2.9	−1.1	0.240	0.05	0.6	0.510	0.05	−1.3	0.166	0.24
Trabecular separation (mm)	0.86±0.14	0.86±0.17	−1.8±7.0	0.90±0.17	0.88±0.15	−1.4±5.5	1.9	0.054	0.12	1.8	0.075	0.12	0.3	0.737	0.05
μFE															
Estimated failure load (N)	−8526.47±2565.85	−9437.76±2405.64[a]	10.3±10.3[b]	−9855.60±2400.04	−9903.59±2425.57	0.1±5.4	8.0	<0.001	0.36	0.7	0.432	0.01	−7.0	<0.001	1.25

Value expressed as mean±SD unless otherwise indicated

[a] $p<0.017$ statistically significant between-sides difference (paired t-test)

[b] $p<0.017$ statistically significant difference in %SSD between-groups (independent t-test)

Abbreviations: *%SSD* percent side-to-side difference, *d* Cohen's d, *vBMD* volumetric bone mineral density, *HA* hydroxyapatite, *N* Newtons, *μFE* finite element analysis

Non-Paretic Distal Tibia (Right)

A **B**

Paretic Distal Tibia (Left)

C **D**

Dominant Distal Tibia (Right)

E **F**

Non-Dominant Distal Tibia (Left)
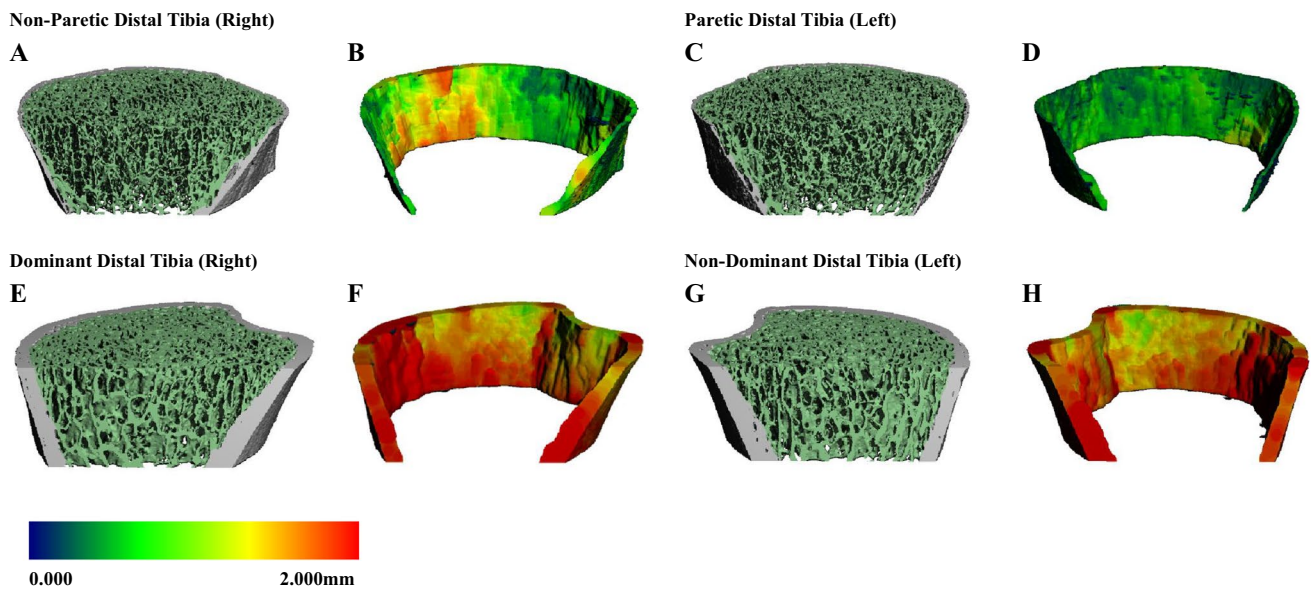
G **H**

0.000 2.000mm

Fig. 1 Bilateral within and between groups comparison of the distal tibia. HR-pQCT generated 3D rendering of the distal tibia for a representative male participant with chronic stroke and an age-matched male control participant (lower panel). The sagittal cut plane was standardized at a depth of 30% with the wider epiphyseal portion of the tibia oriented superiorly and the metaphyseal portion inferiorly. There are comparatively fewer trabeculae with reduced density and network connectivity between the stroke and control participants. Thinning of the cortical shell is also more pronounced on the paretic side compared to the non-paretic side as indicated by a darker spectral color gradient (standardized range 0–2 mm). Bilateral difference in cortical thickness is less pronounced in the control participant. The upper panel shows a bilateral view of the **A** trabecular segment and **B** cortical thickness of the non-paretic tibia compared to the **C** trabecular segment and **D** cortical thickness of the paretic tibia. The lower panel shows the **E** trabecular segment and **F** cortical thickness of the dominant tibia relative to the **G** trabecular segment and **H** cortical thickness of the non-dominant tibia

Discussion

The study results support the stated hypotheses. Side-to-side differences in bone density, cortical area, cortical thickness, and estimated failure load for the distal tibia were more pronounced in the stroke group relative to the control group. Among the various stroke-related impairments, gait speed and spasticity (i.e., 10MWT, CSS-ankle clonus) were independently associated with the %SSD in estimated failure load, after adjusting for the effects of other relevant factors.

Comparison of HR-pQCT variables

The bilateral disparities in vBMD variables observed in the present study are in line with findings from previous pQCT studies of the distal tibia among individuals with stroke [7, 10, 11]. A significant bilateral difference in cortical area (11.6%) was also apparent. Previously, it was difficult to measure cortical variables at distal skeletal sites due to the thin paretic cortical bone shell and the relatively lower resolution of pQCT scanners [26].

A large effect size was evident for %SSD in cortical thickness ($d = 1.29$, $p < 0.001$) suggesting the bilateral disparity was greater for participants with stroke compared to controls. Other microstructural variables showed little difference between sides and groups. The %SSD in cortical thickness (10.9%) was also larger compared to the value reported by Borschmann et al. (4.2%) [22]. The difference in the average time since stroke between our participants (5.8 ± 4.0 years) and those with acute stroke (≤ 6 months) in Borschmann et al. [22] may explain the greater magnitude of %SSD in our study, given the comparatively greater number of cortical remodeling cycles (i.e., approximate average of 18 cycles versus 2 cycles in participants with acute stroke) [28].

Previously, Borschmann et al. also reported significant %SSD in total vBMD, cortical vBMD, and cortical area (at 3.7%, 0.6%, and 4.7%, respectively) [22]. Comparatively, the %SSD in these variables was substantially greater among our participants with chronic stroke (total vBMD, 8.7%; cortical vBMD, 4.1%; cortical area, 11.6%). On the other hand, the %SSD in trabecular vBMD (4.7%) for our participants was similar to their observation (4.8%) [22]. Additional evidence suggests that trabecular bone loss in the paretic tibia is continuous but may plateau approximately 2 years following stroke [8]. While cortical remodeling cycles are comparably shorter, a 2-year duration coincides with the typical remodeling cycle duration of the trabecular bone surface [28]. Taken together, the results suggest that a greater progressive loss of cortical mass/density, relative to trabecular bone, may occur at the distal tibia during the chronic stages of stroke

Table 3 Discriminant analysis of group classification by HR-pQCT variables after adjusting for relevant factors

HR-pQCT variables	Canonical discriminant function summary					Standardized discriminant function coefficients (factors)											(%)^{cv}
	EV	CC	λ	χ²	Sig	1	2	3	4	5	6	7	8	9	10	11	
Discriminant analysis																	
Model 1: Cortical vBMD	1.234	0.743	0.448	97.251	0.000	0.739	-	0.019	0.006	0.008	0.034	-0.040	0.013	-0.052	-0.240	0.847	82.8
Model 2: Estimated failure load	1.205	0.739	0.454	95.669	0.000	-	0.701	0.027	-0.079	0.110	-0.068	-0.047	0.064	-0.039	-0.070	0.825	84.4
Model 3: Cortical vBMD + estimated failure load	1.587	0.783	0.387	114.529	0.000	0.543	0.502	-0.005	-0.020	0.056	0.035	0.002	0.043	0.005	-0.236	0.820	85.2

Dependent variable = group (stroke vs control)

Independent variables = %SSD HR-pQCT variables

Standardized discriminant function coefficients (factors):

Factor 1 = %SSD cortical vBMD, factor 2 = %SSD estimated failure load, factor 3 = sex, factor 4 = age, factor 5 = BMI, factor 6 = PASE, factor 7 = calcium supplementation, factor 8 = tobacco use, factor 9 = alcohol consumption, factor 10 = comorbidities, factor 11 = medications

Abbreviations: χ^2 chi-squared, λ Wilk's Lambda, (%)^{cv} percentage of cross-validated grouped cases correctly classified, %SSD percent side-to-side difference, CC canonical correlation, EV Eigenvalue, vBMD volumetric bone mineral density

recovery (i.e., ≥ 6 months). As this study is cross-sectional in nature, it remains unclear whether cortical bone loss had already reached steady state and will require longitudinal follow-up.

The results are generally similar to previous DXA and pQCT studies demonstrating more compromised bone density and quality in the paretic upper limb than the paretic lower limb [1]. For example, bilateral differences in trabecular bone were less pronounced in the distal tibia reported here when compared with the distal radius previously reported in the same group of people with chronic stroke [23]. Substantially larger %SSD in trabecular vBMD (23.1%) and trabecular microstructure (i.e., trabecular separation = 24.3%) were found for the distal radius [23] than the corresponding values for the distal tibia reported here (trabecular vBMD = 4.7% and trabecular separation = 1.8%). Our previous HR-pQCT study also showed that the %SSD in trabecular vBMD contributed the most to the %SSD in estimated failure load of the distal radius ($\beta = 1.106$) relative to other bone variables [23]. This suggests greater loss of trabecular density in non-weight-bearing than weight-bearing peripheral bone sites during the chronic stages of stroke recovery. Mechanical bone strength parameters (i.e., estimated failure load) also exhibit regional variance, with distal segments being more reflective of total bone strength than proximal segments [29]. Whether our observations of the distal tibia are reflective of concomitant loss of trabecular density in proximal sites (e.g., hip, vertebrae) will require further study.

Gait speed as a determinant of estimated failure load

Slower gait speed was independently associated with greater %SSD in estimated failure load (model 3: $\beta = -0.331$, $p = 0.009$), suggesting impaired walking speed was related to compromised bone strength on the paretic side. Though not analogous, this finding is similar to a previous study in which gait velocity was independently associated with the compressive bone strength index (cBSI) of the paretic tibia ($\beta = -0.379$, $p = 0.001$) [7]. Faster gait velocities may result in higher ground reaction force magnitudes influencing bone remodeling [30] and density in the proximal femur of paretic sides [31]. Slower daily gait speeds have been shown to be predictive of lower daily ambulatory activity post-stroke [32]. Gait speed also affects leg loading during walking, with significantly less paretic side loading observed for individuals with stroke (i.e., home and limited community ambulators) compared to controls at slower walking speeds [33]. Asymmetrical paretic leg weight-bearing also contributes to bone loss post-stroke [34–36]. Higher daily loading frequency during standing and upright activity is associated with slower bone turnover rate between the time of onset and

Table 4 Predictors of %SSD in estimated failure load among individuals with stroke

Predictor	R^2	ΔR^2	ΔF	p (ΔF)	B	β	95% CI		p	VIF
Model 1 (base model)	0.357	0.357	2.359	0.017*						
Sex (0 = male, 1 = female)					6.166	0.297	0.468	11.865	**0.034***	1.486
Age (years)					− 0.357	− 0.269	− 0.769	0.055	0.088	1.891
BMI (kg/m^2)					− 0.555	− 0.165	− 1.462	0.351	0.224	1.424
PASE					− 0.032	− 0.276	− 0.067	0.002	0.062	1.668
Calcium (0 = no, 1 = yes)					− 10.276	− 0.213	− 35.732	15.180	0.421	5.494
Vitamin D (0 = no, 1 = yes)					14.593	0.347	− 6.239	35.425	0.166	4.825
Smoking (0 = no, 1 = yes)					2.462	0.102	− 4.021	8.944	0.449	1.431
Alcohol history (0 = no, 1 = yes)					− 6.834	− 0.277	− 14.552	0.885	0.081	1.932
Total number of comorbidities					4.366	0.546	1.882	6.850	**0.001***	1.898
Total number of medications					− 1.756	− 0.528	− 2.717	− 0.795	**0.001***	1.642
Stroke type (0 = ischemic, 1 = hemorrhagic)					− 7.724	− 0.364	− 13.779	− 1.668	**0.013***	1.602
Time since stroke (years)					-0.188	− 0.073	− 1.011	0.635	0.649	1.989
Model 2	0.451	0.094	8.590	**0.005***						
Base model covariates					-	-	-	-	-	-
10MWT (m/s)					− 9.799	-0.368	− 16.514	− 3.084	**0.005***	1.439
Model 3	0.501	0.050	4.859	**0.032***						
Base model covariates					-	-	-	-	-	-
10MWT (m/s)					− 8.816	− 0.331	− 15.352	− 2.281	**0.009***	1.466
CSS—Ankle Clonus					4.136	0.239	0.365	7.906	**0.032***	1.151

*$p \leq 0.05$ statistically significant

Abbreviations: R^2 total variance, ΔR^2 additional predictor variance, ΔF F-value change, *B* unstandardized regression coefficient, *β* standardized regression coefficient, *95%CI* 95% confidence interval, *%SSD* percent side-to-side difference, *10MWT* 10-m walk test, *BMI* body mass index, *CSS-ankle clonus* Composite Spasticity Scale-ankle clonus, *PASE* Physical Activity Scale for the Elderly, *VIF* variance inflation factor

6 months post-stroke [22]. Therefore, having slower walking speeds, lower ambulatory activity, and reduced leg loading during the walking cycle may, in combination, adversely affect bone quality in the lower limbs, particularly on the paretic side.

Although bone status is influenced by a number of non-modifiable cofactors (e.g., other significant base model correlates in the regression analysis such as sex, comorbidity, and stroke type), the fact that individual factors such as spasticity and gait speed, both modifiable, could contribute to an additional 5.0% and 9.4% of the variance in estimated failure load may be clinically important. An intervention program which incorporates simple gait exercises to enhance walking speed is both economical and clinically feasible when considering the time commitment and resources required to promote even relatively small improvements in bone strength (e.g., roughly 9–10%). Early ambulation and structured group exercise interventions have been shown to play an important role in maintaining bone strength and possibly reducing fracture risk after stroke [1, 37]. Treadmill walking interventions produced modest improvements in tibial bone geometry among people with stroke [6]. Comprehensive, multicomponent community-based fitness and mobility programs have also been shown to increase cortical BMD and

cortical thickness in the tibial diaphysis after stroke [9, 38]. The dosage of gait and mobility training at different stages of stroke recovery remain the subject of further study.

Spasticity as a determinant of estimated failure load

The CSS subscale score for sustained ankle clonus was independently associated with %SSD in estimated failure load in the regression model (model 3: $\beta = 0.239$, $p = 0.032$). Whether certain CSS subscales assessing neurogenic presentations of spasticity (i.e., ankle clonus, Achilles tendon jerk) had a predominate influence in their association with %SSD in estimated failure load over other scale components assessing both neurogenic and non-neurogenic factors (i.e., resistance to passive joint displacement) due to exaggerated stretch reflex and alterations in muscle mechanical properties is unclear. Consensus regarding the impact of spasticity on post-stroke bone status is currently lacking, as correlations are inconsistent across studies [5, 7, 10, 12, 23, 26, 39, 40].

The ability to assess diverse presentations of spasticity is a methodological limitation of previous studies. The Modified Ashworth Scale is only used to evaluate resistance to joint displacement during passive elbow extension or ankle dorsiflexion. By contrast, the CSS is a comprehensive,

multi-component scale. A study of the distal tibia metaphysis showed that spasticity was associated with multiple bone variables (i.e., total bone mineral content, total density, trabecular density, and bone strength index) ($p < 0.05$), and moderate to severe spasticity was independently associated with the bone strength index ($\beta = -0.235$, $p = 0.028$) [7]. Yet in another study of the tibia midshaft, spasticity and bone strength index showed no significant correlation (men, $r = -0.167$; women, $r = -0.014$) [5]. For investigating the impact of spasticity on bone, future studies should consider the precision of the assessment used. With regard to potential interventions, recent meta-analyses suggest that transcutaneous electrical nerve stimulation (TENS) may be an effective treatment for reducing lower limb spasticity post-stroke [41, 42]. The use of TENS is also a relatively economical and easily administered therapy. Additional studies are needed which substantiate the direct or indirect effect of TENS therapy for improving bone health after stroke.

Limitations

There are several limitations with regards to the scanning procedures and study design used. The standard µFE analysis with a uniform linear modulus was used for all participants. With non-linear approaches, cortical and trabecular bone elements are assigned to different moduli [43]. Values also differ based on modulus direction [44], with non-linear approaches rendering more direct mechanical bone strength estimations. However there is also support for the use of linear approaches [43]. Due to the lower vBMD, cortical area, and cortical thickness relative to trabecular parameters observed in this study, a non-linear approach may be useful in assessing bilateral as well as compartmental disparities in bone post-stroke.

Estimated failure load derived from the µFE analysis was the primary outcome of this study. This parameter may be of particular importance in clinical trials where estimated bone strength is the primary target of treatment or therapy rather than changes in individual bone parameters (i.e., density, area) which may require longer follow-up and larger sample sizes [45]. Although µFE measures have been shown to be relatively stronger predictors of incident fractures and bone strength than other HR-pQCT parameters in validation studies [29, 46] and at the cohort level in vivo [21], ex vivo simulations are conducted using cadaver segments which are not subject to motion artifact. The precision of µFE measures for determining fracture-associated changes at the individual level demonstrates room for improvement (least significant change (LSC) $\geq 5\%$) [47]. Standardization of applied models (i.e., modulus assignment, segmentation and boundary conditions, yield criterion) [24], correction values [48], and registration methods (i.e., cross-sectional,

3D) [49] may be important for improving the relative precision of µFE measures for future studies among participants with stroke.

A standardized fixed offset distance was used for determining the scan region across all participants. Standardization using this approach is considered an acceptable method and has been used in previous studies comparing diabetic postmenopausal women to controls [50] and in large, multicenter cohort trials [21]. Although several other studies have also used this method [16–18, 51], a relative offset distance approach, even with its own inherent limitations, considers individual limb length differences across subjects [24].

Additionally, our regression model identified only two stroke impairment variables that were independently associated with estimated failure load. The magnitude of the correlations observed was also weak. This suggests that a larger sample size is needed to build a more comprehensive prediction model. There are also limitations in the generalizability of the findings due to study design. All participants from the stroke and control groups were recruited through a non-probability sampling method and may unintentionally exclude individuals with diverse clinical presentations. Furthermore, the study was a cross-sectional design and therefore cannot provide a causal link between the impairments previously described and fracture risk after stroke.

Conclusion

The paretic distal tibia showed more compromised bone density, cortical area, cortical thickness, and estimated failure load than the non-paretic distal tibia. Although weak in magnitude, gait speed and spasticity were significant clinical correlates of the side-to-side difference in estimated failure load that were independent of largely non-modifiable cofactors (e.g., sex, comorbidity, stroke type). As treatment programs focusing on these potentially modifiable stroke-related impairments are feasible to administer, future studies are needed to determine the efficacy of such intervention strategies for improving bone strength in individuals with chronic stroke.

Declarations

Ethics approval Ethical approval was obtained from the Human Research Ethics Review Committee of the University. All of the experimental procedures were conducted in accordance with the Helsinki Declaration for human experiments.

Consent to participate The details of the study were explained to the participants before informed written consent was obtained.

Consent for publication Consent to use information and data collected during the course of the study for educational and knowledge dissemination purposes was granted by the participants.

Conflicts of interest None.

References

1. Eng JJ (2008) Balance, falls, and bone health: Role of exercise in reducing fracture risk after stroke. J Rehabil Res Dev 45:297–314
2. Poole KES, Reeve J, Warburton EA (2002) Falls, fractures, and osteoporosis after stroke. Time to think about protection? Stroke 33:1432–1436
3. Dennis MS, Lo KM, McDowall M, West T (2002) Fractures after stroke Frequency, Types, and Associations. Stroke 33:728–734
4. Ramnemark A, Nyberg L, Borssén B, Olsson T, Gustafson Y (1998) Fractures after stroke. Osteoporos Int 8:92–95
5. Pang MY, Ashe MC, Eng JJ (2008) Tibial bone geometry in chronic stroke patients: influence of sex, cardiovascular health, and muscle mass. J Bone Miner Res 23:1023–1030
6. Pang MYC, Lau RWK (2010) The effects of treadmill exercise training on hip bone density and tibial bone geometry in stroke survivors: a pilot study. Neurorehabil Neural Repair 24:368–376
7. Pang MY, Ashe MC, Eng JJ (2010) Compromised bone strength index in the hemiparetic distal tibia epiphysis among chronic stroke patients: the association with cardiovascular function, muscle atrophy, mobility, and spasticity. Osteoporos Int 21:997–1007
8. Lam FM, Bui M, Yang FZ, Pang MY (2016) Chronic effects of stroke on hip bone density and tibial morphology: a longitudinal study. Osteoporos Int 27:591–603
9. Pang MYC, Ashe MC, Eng JJ, McKay HA, Dawson AS (2006) A 19-week exercise program for people with chronic stroke enhances bone geometry at the tibia: a peripheral quantitative computed tomography study. Osteoporos Int 17:1615–1625
10. Yang FZ, Pang MY (2015) Influence of chronic stroke impairments on bone strength index of the tibial distal epiphysis and diaphysis. Osteoporos Int 26:469–480
11. Talla R, Galea M, Lythgo N, Eser T, Talla P, Angeli P, Eser P, Lythgo P (2011) Contralateral comparison of bone geometry,

12. Lazoura O, Groumas N, Antoniadou E, Papadaki PJ, Papadimitriou A, Thriskos P, Fezoulidis I, Vlychou M (2008) Bone mineral density alterations in upper and lower extremities 12 months after stroke measured by peripheral quantitative computed tomography and DXA. J Clin Densitom 11:511–517
13. Ramnemark A, Nyberg L, Lorentzon R, Englund U, Gustafson Y (1999) Progressive hemiosteoporosis on the paretic side and increased bone mineral density in the nonparetic arm the first year after severe stroke. Osteoporos Int 9:269–275
14. Souzanchi MF, Palacio-Mancheno P, Borisov YA, Cardoso L, Cowin SC (2012) Microarchitecture and bone quality in the human calcaneus: local variations of fabric anisotropy. J Bone Miner Res 27:2562–2572
15. Boutroy S, Bouxsein ML, Munoz F, Delmas PD (2005) In vivo assessment of trabecular bone microarchitecture by high-resolution peripheral quantitative computed tomography. J Clin Endocrinol Metab 90:6508–6515
16. Burt LA, Manske SL, Hanley DA, Boyd SK (2018) Lower bone density, impaired microarchitecture, and strength predict future fragility fracture in postmenopausal women: 5-year follow-up of the Calgary CaMos Cohort. J Bone Miner Res 33:589–597
17. Sornay-Rendu E, Boutroy S, Duboeuf F, Chapurlat RD (2017) Bone microarchitecture assessed by HR-pQCT as predictor of fracture risk in postmenopausal women: the OFELY study. J Bone Miner Res 32:1243–1251
18. Szulc P, Boutroy S, Chapurlat R (2018) Prediction of fractures in men using bone microarchitectural parameters assessed by high-resolution peripheral quantitative computed tomography-the prospective STRAMBO Study. J Bone Miner Res 33:1470–1479
19. Langsetmo L, Peters KW, Burghardt AJ et al (2018) Volumetric bone mineral density and failure load of distal limbs predict incident clinical fracture independent of FRAX and clinical risk factors among older men. J Bone Miner Res 33:1302–1311
20. Fink HA, Langsetmo L, Vo TN, Orwoll ES, Schousboe JT, Ensrud KE, Osteoporotic Fractures in Men Study G (2018) Association of high-resolution peripheral quantitative computed tomography (HR-pQCT) bone microarchitectural parameters with previous clinical fracture in older men: the Osteoporotic Fractures in Men (MrOS) study. Bone 113:49–56
21. Samelson EJ, Broe KE, Xu H et al (2019) Cortical and trabecular bone microarchitecture as an independent predictor of incident fracture risk in older women and men in the Bone Microarchitecture International Consortium (BoMIC): a prospective study. Lancet Diabetes Endocrinol 7:34–43
22. Borschmann K, Iuliano S, Ghasem-Zadeh A, Churilov L, Pang MYC, Bernhardt J (2018) Upright activity and higher motor function may preserve bone mineral density within 6 months of stroke: a longitudinal study. Arch Osteoporos 13:5
23. Miller T, Ying MTC, Hung VWY, Tsang CSL, Ouyang H, Chung RCK, Qin L, Pang MYC (2020) Determinants of estimated failure load in the distal radius after stroke: An HR-pQCT study. Bone 144:115831
24. Whittier DE, Boyd SK, Burghardt AJ, Paccou J, Ghasem-Zadeh A, Chapurlat R, Engelke K, Bouxsein ML (2020) Guidelines for the assessment of bone density and microarchitecture in vivo using high-resolution peripheral quantitative computed tomography. Osteoporos Int 31(9):1607–1627
25. Portney LG (2015) Foundations of clinical research : applications to practice. F.A. Davis Company, Philadelphia
26. Pang MY, Cheng AQ, Warburton DE, Jones AY (2012) Relative impact of neuromuscular and cardiovascular factors on bone strength index of the hemiparetic distal radius epiphysis among individuals with chronic stroke. Osteoporos Int 23:2369–2379

27. Blanca MJ, Alarcon R, Arnau J, Bono R, Bendayan R (2017) Non-normal data: is ANOVA still a valid option? Psicothema 29:552–557

28. Eriksen EF (2010) Cellular mechanisms of bone remodeling. Rev Endocr Metab Disord 11:219–227

29. Zhou B, Zhang Z, Hu Y, Wang J, Yu YE, Nawathe S, Nishiyama KK, Keaveny TM, Shane E, Guo XE (2019) Regional variations of HR-pQCT morphological and biomechanical measurements of the distal radius and tibia and their associations with whole bone mechanical properties. J Biomech Eng 141(9):0910081–0910087

30. Barry DW, Kohrt WM (2008) Exercise and the preservation of bone health. J Cardiopulm Rehabil Prev 28:153–162

31. Worthen LC, Kim CM, Kautz SA, Lew HL, Kiratli BJ, Beaupre GS (2005) Key characteristics of walking correlate with bone density in individuals with chronic stroke. J Rehabil Res Dev 42:761–768

32. Fulk GD, He Y, Boyne P, Dunning K (2017) Predicting home and community walking activity poststroke. Stroke 48:406–411

33. Raja B, Neptune RR, Kautz SA (2012) Quantifiable patterns of limb loading and unloading during hemiparetic gait: relation to kinetic and kinematic parameters. J Rehabil Res Dev 49:1293–1304

34. Jørgensen L, Crabtree NJ, Reeve J, Jacobsen BK (2000) Ambulatory level and asymmetrical weight bearing after stroke affects bone loss in the upper and lower part of the femoral neck differently: bone adaptation after decreased mechanical loading. Bone 27:701–707

35. Chang K-H, Liou T-H, Sung J-Y, Wang C-Y, Genant HK, Chan WP (2014) Femoral neck bone mineral density change is associated with shift in standing weight in hemiparetic stroke patients. Am J Phys Med Rehabil 93:477–485

36. Sherk KA, Sherk VD, Anderson MA, Bemben DA, Bemben MG (2013) Differences in tibia morphology between the sound and affected sides in ankle-foot orthosis-using survivors of stroke. Arch Phys Med Rehabil 94:510–515

37. Eng JJ (2010) Fitness and Mobility Exercise (FAME) Program for stroke. Top Geriatr Rehabil 26:310–323

38. Pang MYC, Eng JJ, Dawson AS, McKay HA, Harris JE (2005) A community-based fitness and mobility exercise program for older adults with chronic stroke: a randomized, controlled trial. J Am Geriatr Soc 53:1667–1674

39. Pang MY, Ashe MC, Eng JJ (2007) Muscle weakness, spasticity and disuse contribute to demineralization and geometric changes in the radius following chronic stroke. Osteoporos Int 18:1243–1252

40. Pang MY, Eng JJ (2005) Muscle strength is a determinant of bone mineral content in the hemiparetic upper extremity: implications for stroke rehabilitation. Bone 37:103–111

41. Marcolino MAZ, Hauck M, Stein C, Schardong J, Pagnussat AdS, Plentz RDM (2020) Effects of transcutaneous electrical nerve stimulation alone or as additional therapy on chronic post-stroke spasticity: systematic review and meta-analysis of randomized controlled trials. Disabil Rehabil 42:623–635

42. Lin S, Sun Q, Wang H, Xie G (2018) Influence of transcutaneous electrical nerve stimulation on spasticity, balance, and walking speed in stroke patients: a systematic review and meta-analysis. J Rehabil Med 50:3–7

43. Macneil JA, Boyd SK (2008) Bone strength at the distal radius can be estimated from high-resolution peripheral quantitative computed tomography and the finite element method. Bone 42:1203–1213

44. Turner CH, Rho J, Takano Y, Tsui TY, Pharr GM (1999) The elastic properties of trabecular and cortical bone tissues are similar: results from two microscopic measurement techniques. J Biomech 32:437–441

45. van Rietbergen B, Ito K (2015) A survey of micro-finite element analysis for clinical assessment of bone strength: the first decade. J Biomech 48:832–841

46. Varga P, Dall'Ara E, Pahr DH, Pretterklieber M, Zysset PK (2011) Validation of an HR-pQCT-based homogenized finite element approach using mechanical testing of ultra-distal radius sections. Biomech Model Mechanobiol 10:431–444

47. Mikolajewicz N, Bishop N, Burghardt AJ et al (2019) HR-pQCT measures of bone microarchitecture predict fracture: systematic review and meta-analysis. J Bone Miner Res 35(3):446–459

48. Zhou B, Wang J, Yu YE, Zhang Z, Nawathe S, Nishiyama KK, Rosete FR, Keaveny TM, Shane E, Guo XE (2016) High-resolution peripheral quantitative computed tomography (HR-pQCT) can assess microstructural and biomechanical properties of both human distal radius and tibia: ex vivo computational and experimental validations. Bone 86:58–67

49. Ellouz R, Chapurlat R, van Rietbergen B, Christen P, Pialat J-B, Boutroy S (2014) Challenges in longitudinal measurements with HR-pQCT: evaluation of a 3D registration method to improve bone microarchitecture and strength measurement reproducibility. Bone 63:147–157

50. Patsch JM, Burghardt AJ, Yap SP, Baum T, Schwartz AV, Joseph GB, Link TM (2013) Increased cortical porosity in type 2 diabetic postmenopausal women with fragility fractures. J Bone Miner Res 28:313–324

51. Zhu TY, Hung VW, Cheung WH, Cheng JC, Qin L, Leung KS (2016) Value of measuring bone microarchitecture in fracture discrimination in older women with recent hip fracture: a case-control study with HR-pQCT. Sci Rep 6:34185